Ti nanorod arrays with periodic density fabricated via anodic technology

Meiling Zhong[1], Jingwen Liao[1], Guoxin Tan[2], Yu Zhang[3], Xi Lin[3], Peng Yu[1], Zunxiong Yu[1], Chengyun Ning[1]

[1]*School of Materials Science and Engineering, South China University of Technology, Guangzhou 510641, People's Republic of China*
[2]*Institute of Chemical Engineering and Light Industry, Guangdong University of Technology, Guangzhou 510006, People's Republic of China*
[3]*General Hospital of Guangzhou Military Command of PLA, Guangzhou 510010, People's Republic of China*
E-mail: ning_lab@hotmail.com

Published in Micro & Nano Letters; Received on 26th September 2013; Revised on 21st December 2013; Accepted on 28th January 2014

Fabrication of the anodic metals nanorod, especially Ti (titanium) nanorod arrays (Ti-NRAs), has attracted increasing attention in recent years. In this reported work, Ti-NRAs were prepared by applying a constant current of 200 mA under different anodisation conditions. The field emission scanning electron microscopy results showed that the density of the Ti-NRAs could be periodically tuned by the conditions of electrochemical anodisation. A possible formation mechanism is proposed to demonstrate the periodical tuning of the Ti-NRAs' density by the electrochemical anodisation time. This well-controlled synthesis approach may shed light on the fabrication of similar nanostructures of other metal materials.

1. Introduction: Enormous research efforts have been dedicated to the design and the synthesis of nanostructures with controllable morphologies, mainly owing to their specific surface area and biological properties that ensure their promising applications for sensors, photocatalytic reactions and biomedical devices [1–3]. Tuning a specific nanostructure allows a more precise control of the material properties [4, 5]. For example, through conversion from the TiO_2 nanorod arrays to the TiO_2 nanotube arrays by hydrothermal etching, the conversion efficiency of the quantum dye-sensitised solar cells increased by 60% [6]. The ZnO nanorods and the nanowires showed a higher sensitivity of the ethanol sensor compared with the ZnO nanotubes [7]. Recently, the effects of the controllable nanorod arrays' density on the material properties have been investigated in some studies for further studying the performances of nanorod arrays [8, 9]. Wang's group reported a systematic study on the density-controlled hydrothermal growth of ZnO nanorod arrays by controlling the substrate pre-treatment conditions [10]. Park and co-workers found that the length and the density of the ZnO nanorod arrays were controlled by the time of the thermal chemical vapour deposition, and the properties of the green emission intensity could be finely controlled by tuning the ZnO nanorod arrays' density [11]. Nevertheless, the density of the Ti-NRAs has been investigated rarely. Ti and its alloys have been extensively used as orthopaedic and dental implants over recent decades because of their generally excellent biocompatibility, good corrosion resistance and high machinability [12]. The special nanoscale topography of titanium is an important factor for bone repairing materials, which plays a significant role in protein adsorption, cell adhesion, migration and differentiation [13]. To date, great progress has been made in the growth of Ti-based nanostructures with tunable sizes. The research demonstrated that 15 nm-high nanorod arrays resulted in the greatest cell response [14]. In our group, we have previously described the nanostructure (nanotube, nanorod and nanoflake) transition on the anodic Ti and reported that the length of the Ti-NRAs could be tuned via the electrochemical anodisation time [15, 16]. However, the density of the Ti-NRAs' has not been considered.

This Letter aims to demonstrate that the Ti-NRAs' density is controllable by selective corrosion growth on the Ti substrate. This Letter's results demonstrate that the Ti-NRAs' density could be tuned periodically by tailoring the electrochemical anodisation time. Furthermore, other experimental conditions such as the pH value of the electrolyte, the concentration of the fluoride ion and the temperature of the electrolyte and so on, also had an important influence on the resulting Ti-NRAs' density.

2. Experimental: Ti foil (0.2 mm thick, obtained according to the standard ASTM F67-2002 for a biomedical application, Baoji Qichen New Material Technology Co. Ltd) was degreased by sonicating in acetone and ethanol, treated with 1:1 (v/v) HF and HNO_3 solution, followed by rinsing with deionised water and drying in the air. Electrochemical anodisation was conducted in a two-electrode configuration, where the Ti and the Cu foils worked as the working and the counter electrodes, respectively, and a mixture of 1.45 wt% NH_4F and 1.93 wt% $H_2C_2O_4$ was used as the electrolyte. Before the electrochemical treatment, the Ti foil was placed in the electrolyte for 10 min. Anodisation was performed by applying a constant current of 200 mA for different times at room temperature via a DC power supply. The as-prepared specimens were washed with deionised water.

Electron probe micro-analysis (EPMA) was performed to compare the elements of the nanorods and the foil, respectively. Field emission scanning electron microscopy (FE-SEM, Nova Nano SEM 430, Germany) was employed to characterise the morphology of the Ti-NRAs.

3. Results and discussion: The EPMA was used to compare the composition of the nanorods with the Ti foil. The EPMA results shown in Fig. 1 reveal that only the Ti element could be detected on the nanorods' surface. Similarly, Ti was the dominating element in the foil, and the presence of trace amounts of the C and the O elements could be attributed to the thin film of the titanium oxide formed in the interface with air. It was indicated that the nanorods shared the same chemical component with the foil.

A particularly interesting feature of the Ti-NRAs during a galnostatic anodisation was that the Ti-NRAs' density could be adjusted periodically by a manipulation of the anodisation time. Fig. 2*a* depicts the relative density of the Ti-NRAs over the time period of 10–130 min. It was apparent that the average Ti-NRAs'

© The Institution of Engineering and Technology 2014

doi: 10.1049/mnl.2013.0565

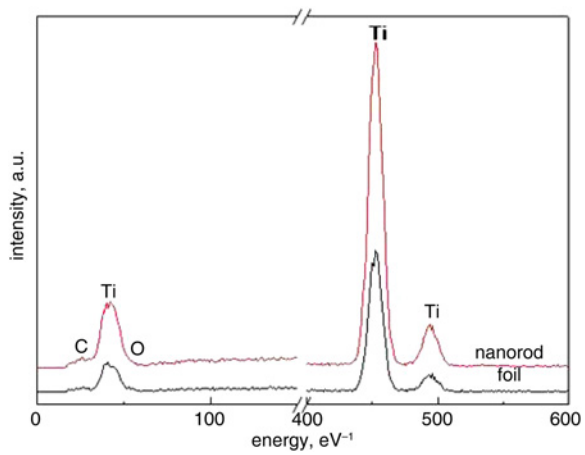

Figure 1 *EPMA profiles of nanorods and Ti foil*

density was considered as zero at 15 min, reached the maximum density at 40 min and the minimum density at 75 min, which was namely called 'cycle', while the second cycle occurred in the range of 80–125 min with the maximum density at 100 min. The density of the Ti-NRAs decreased at 130 min, in comparison to those at 125 min, implying the start of a new cycle. Figs. 2*b*1–*b*9 shows the FE-SEM images of the Ti-NRAs obtained at the anodisation times of 15, 20, 40, 50, 75, 80, 100, 110 and 125 min, illustrating that the changing trend of the Ti-NRAs' density was presented in a vivid way. As a straightforward proof, the Ti foil was etched thinner and thinner in the whole process.

In addition to the anodisation time, other experimental conditions such as the pH value of the electrolyte, the current amplitude, the concentration of the fluoride ion and the temperature of the electrolyte and so on, also had an important influence on the Ti-NRAs' morphologies. For example, when the pH of the electrolyte increased from 4.32 to around 5.2 by reducing the concentration of $H_2C_2O_4$, the density of the Ti-NRAs decreased, which indicated that the H^+ had an important effect on the Ti-NRAs' density. Fig. 3 shows the FE-SEM images of the Ti-NRAs with the diverse densities obtained by anodisation of the Ti foil in the electrolyte of the different pH values. The Ti-NRAs' density increased with decrease of the pH of the electrolyte. The Ti-NRAs' densities were calculated as $(0.88 \pm 0.02) \times 10^{10}$ /cm^2, $(1.79 \pm 0.04) \times 10^{10}$ /cm^2 and $(4.51 \pm 0.06) \times 10^{10}$ /cm^2, respectively. The density of the Ti-NRAs was

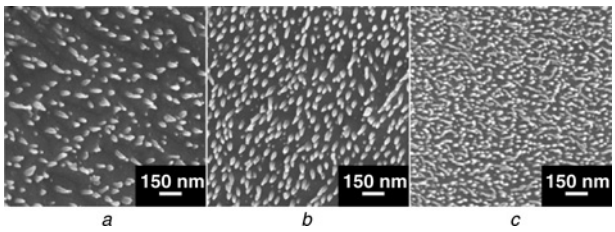

Figure 3 *FE-SEM images of Ti-NRAs*
Nanorods samples were prepared by applying a constant current of 200 mA for 30 min in aqueous electrolyte containing 1.45 wt% NH_4F and 0.48 wt%, 0.72 wt%, 1.93 wt% $H_2C_2O_4$
a 0.48 wt%
b 0.72 wt%
c 1.93 wt% $H_2C_2O_4$

calculated by converting the nanorods number in 500 nm^2 of the six random areas on the FE-SEM image.

In our earlier Letters [15, 16] on the formation of Ti-NRAs and nanotubes, it has already been elucidated that the Ti-NRAs grow as a result of a competition between the electrochemical oxidation of TiO_2 and the chemical corrosion of the Ti foil by F^-, as shown in (1) and (2). Therefore a mechanism (Fig. 4) is proposed to demonstrate the periodic density tuned by the anodisation time

$$\mathrm{Ti} + 2\mathrm{H_2O} \rightarrow \mathrm{TiO_2} + 4\mathrm{H^+} + 4\mathrm{e^-} \quad (1)$$

$$\mathrm{TiO_2} + 4\mathrm{H^+} + 6\mathrm{F^-} \rightarrow \mathrm{TiF_6^{2-}} + 2\mathrm{H_2O} \quad (2)$$

In the first stage (Fig. 4*a*), the Ti substrate is immersed in the electrolyte for 10 min before anodisation. Since the initial reaction rate of the chemical etching is larger than that of the oxidation, the unordered Ti-NRAs are formed, and the thickness of the Ti foil is (186 ± 2.3) μm before the anodisation. In the second stage (Fig. 4*b*), when the anodisation starts, the chemical corrosion of the Ti-NRAs on the Ti substrate results in the disappearance of the Ti-NRAs. Moreover, the Ti foil is etched thinner at 15 min, which is (155 ± 1.9) μm. In the third stage (Fig. 4*c*), the thickness of the Ti foil is (147 ± 1.6) μm at 20 min, the Ti-NRAs grow as the dissolution rate of the substrate is greatly enhanced at the Ti foil bottom and the ordered nanorod arrays are prepared via a selection process. Meanwhile, the growth rate of the Ti-NRAs is different,

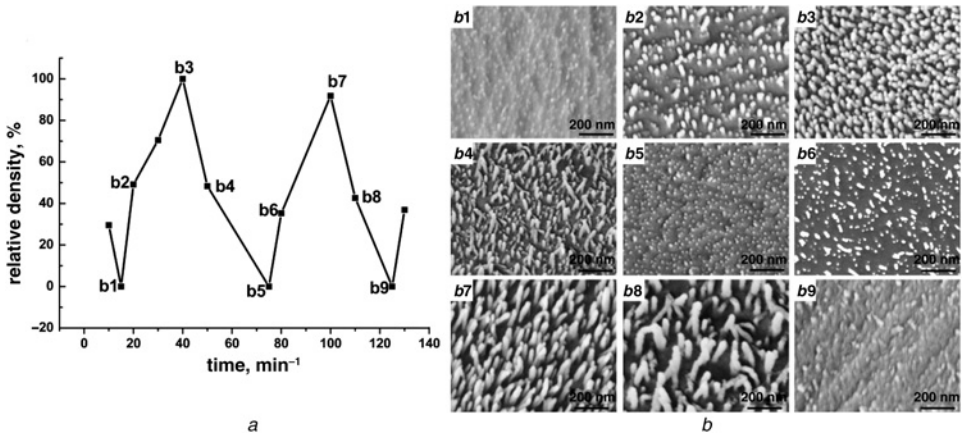

Figure 2 *Relative density of Ti-NRAs fabricated by anodisation within time period of 10–130 min, and FE-SEM images of Ti-NRAs obtained at 15, 20, 40, 50, 75, 80, 100, 110, 125 min*
a Relative density of Ti-NRAs fabricated by anodisation within time period of 10–130 min
Average Ti-NRAs density obtained at 40 min was assumed as 100%, and relative densities of Ti-NRAs obtained at other times were defined as the ratio between the real density of Ti-NRAs at other times and that at 40 min
b FE-SEM images of Ti-NRAs obtained at 15 (*b*1), 20 (*b*2), 40 (*b*3), 50 (*b*4), 75 (*b*5), 80 (*b*6), 100 (*b*7), 110 (*b*8), 125 (*b*9) min

© The Institution of Engineering and Technology 2014

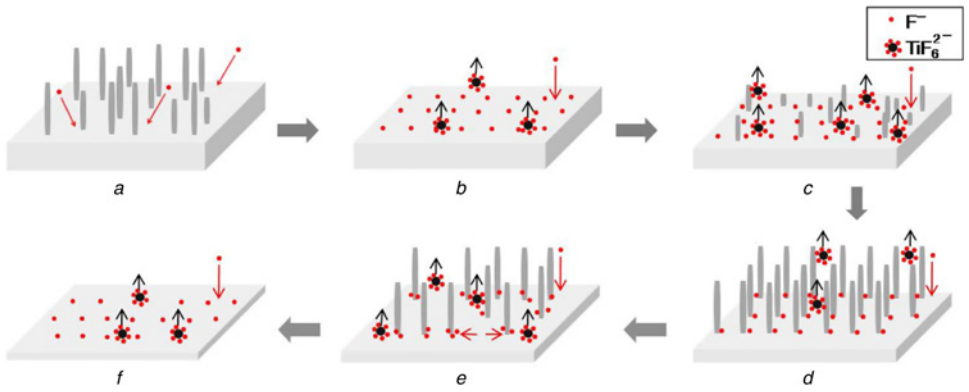

Figure 4 *Schematic illustration of Ti-NRAs' controllable density*

which leads to the formation of the Ti-NRAs with a diverse length, and the Ti-NRAs' density increases. In the fourth stage (Fig. 4*d*), the thickness of the Ti foil is (121 ± 1.8) μm at 40 min, the Ti-NRAs are gradually generated longer and new Ti-NRAs continue to be formed because of the chemical etching of the Ti substrate, resulting in the increase of the Ti-NRAs' density. However, in the fifth stage (Fig. 4*e*), the thickness of the Ti foil is (110 ± 1.5) μm at 50 min, and it is observed that the Ti-NRAs detach from the Ti substrate, and then the Ti-NRAs collapsed gradually. It should be explained that the chemical corrosion rate of the Ti-NRAs from the bottom is enhanced, which is due to the accumulation of the mass-transfer process of F^- from the solution to the Ti-NRAs' bottom along with the increase of the Ti-NRAs' density. Therefore the density of the Ti-NRAs declines. In the last stage (Fig. 4*f*), when the F^- etching rate on the Ti-NRAs' bottom is far larger than that in the other positions, the Ti-NRAs nearly disappear, which implies the beginning of a new cycle. What is more, the Ti foil is etched to be very thin and the thickness of the Ti foil is (80 ± 1.3) μm at 75 min.

4. Conclusion: Ti-NRAs have been fabricated via a selective corrosion of the Ti substrate by using the electrochemical anodisation technique. Control of the periodic Ti-NRAs' density was feasible by tuning the anodisation time. Moreover, a mechanism is proposed to interpret the controllability of the periodic Ti-NRAs' density, which is mainly caused by the F^- etch rate of the Ti substrate and the Ti-NRAs. The density of the Ti-NRAs increases as the dissolution rate of the Ti substrate is greatly enhanced, and decreases as the corrosion rate of the Ti-NRAs from the bottom is enhanced. The Ti-NRAs with a tunable density have potential fine applications in biomaterial and photocatalytic reactions and so on.

5. Acknowledgments: The authors gratefully acknowledge the financial support of the National Basic Research Program of China (grant no. 2012CB619100) and the National Natural Science Foundation of China (grant nos 51372087 and 51072057).

M. Zhang and J. Liao both contributed equally.

6. References

[1] Guo S., Wang E.: 'Noble metal nanomaterials: controllable synthesis and application in fuel cells and analytical sensors', *Nano Today*, 2011, **6**, pp. 240–264

[2] Guo S., Wang E.: 'Functional micro/nanostructures: simple synthesis and application in sensors, fuel cells, and gene delivery', *Acc. Chem. Res.*, 2011, **44**, pp. 491–500

[3] Bavykin D.V., Friedrich J.M., Walsh F.C.: 'Protonated titanates and TiO_2 nanostructured materials: synthesis, properties, and applications', *Adv. Mater.*, 2006, **18**, pp. 2807–2824

[4] Jiang Y., Wu M., Wu X., Sun Y., Yin H.: 'Low-temperature hydrothermal synthesis of flower-like ZnO microstructure and nanorod array on nanoporous TiO_2 film', *Mater. Lett.*, 2009, **63**, pp. 275–278

[5] Li Y., Yang X.-Y., Feng Y., Yuan Z.-Y.: 'One-dimensional metal oxide nanotubes, nanowires, nanoribbons, and nanorods: synthesis, characterizations, properties and applications', *Crit. Rev. Solid State Mater. Sci.*, 2012, **37**, pp. 1–74

[6] Huang H., Pan L., Lim C.K., *ET AL.*: 'Hydrothermal growth of TiO_2 nanorod arrays and in situ conversion to nanotube arrays for highly efficient quantum dot-sensitized solar cells', *Small*, 2013, **9**, pp. 3153–3160

[7] Rout C.S., Hari Krishna S., Vivekchand S., Govindaraj A., Rao C.: 'Hydrogen and ethanol sensors based on ZnO nanorods, nanowires and nanotubes', *Chem. Phys. Lett.*, 2006, **418**, pp. 586–590

[8] Tay C., Le H., Chua S., Loh K.: 'Empirical model for density and length prediction of ZnO nanorods on Gan using hydrothermal synthesis', *J. Electrochem. Soc.*, 2007, **154**, pp. K45–K50

[9] Le H., Chua S., Koh Y., Loh K., Fitzgerald E.: 'Systematic studies of the epitaxial growth of single-crystal ZnO nanorods on Gan using hydrothermal synthesis', *J. Cryst. Growth*, 2006, **293**, pp. 36–42

[10] Ma T., Guo M., Zhang M., Zhang Y., Wang X.: 'Density-controlled hydrothermal growth of well-aligned ZnO nanorod arrays', *Nanotechnology*, 2007, **18**, p. 035605

[11] Bae S.Y., Seo H.W., Choi H.C., Park J.: 'Heterostructures of ZnO nanorods with various one-dimensional nanostructures', *T. Phys. Chem. B*, 2004, **108**, pp. 12318–12326

[12] He G., Liu P.: 'Porous titanium materials with entangled wire structure for load-bearing biomedical applications', *J. Mech. Behav. Biomed. Mater.*, 2012, **5**, pp. 16–31

[13] Wang H.-J., Sun Y.-Y., Cao Y., *ET AL.*: 'Is there an optimal topographical surface in nano-scale affecting protein adsorption and cell behaviors? Part II', *J. Nanoparticle Res.*, 2012, **14**, pp. 1–10

[14] Sjöström T., Dalby M.J., Hart A., *ET AL.*: 'Fabrication of pillar-like titania nanostructures on titanium and their interactions with human skeletal stem cells', *Acta Biomater.*, 2009, **5**, pp. 1433–1441

[15] Huang S., Ning C., Peng W., Dong H.: 'Anodic formation of Ti nanorods with periodic length', *Electrochem. Commun.*, 2012, **17**, pp. 14–17

[16] Huang S., Peng W., Ning C., Hu Q., Dong H.: 'Nanostructure transition on anodic titanium: structure control via a competition strategy between electrochemical oxidation and chemical etching', *J. Phys. Chem. C*, 2012, **116**, pp. 22359–22364

© The Institution of Engineering and Technology 2014

doi: 10.1049/mnl.2013.0565